

INTEREST OF IN SITU-RAMAN SPECTROSCOPY IN THE OPTIMIZATION OF PIEZOELECTRIC FIBERS FOR THE DEVELOPMENT OF ENERGY HARVESTERS.

François Rault¹, David Chapron^{2,3}, Anaëlle Talbourdet¹, Cédric Cochrané¹, Guillaume Lemort¹, Eric Devaux¹, Christine Campagne¹, Patrice Bourson^{2,3}

¹ ENSAIT, GEMTEX - Laboratoire de Génie et Matériaux Textiles, F-59000 Lille, France

² Université de Lorraine, Laboratoire Matériaux Optiques Photoniques et Systèmes (LMOPS), Metz, F-57070, France

³ Supélec, Laboratoire Matériaux Optiques Photoniques et Systèmes (LMOPS), Metz, F-57070, France
francois.rault@ensait.fr

ABSTRACT

Energy harvesting is a promising concept that can be used in the development of smart textiles to solve one of the major issues: energy supply. Producing PVDF piezoelectric fibers is a possible way. However, to ensure the piezoelectric character and lead an electromechanical conversion its β phase is needed. The modification of crystalline phases is linked to the processing parameters. In-situ Raman spectroscopy measurements are made on a spinning device used for new synthetic fibers developments or small productions. The content of the crystalline phases α and β is measured for the first time at key points of such process.

Key Words: PVDF, melt-spinning, β phase, in-situ characterization, Raman spectroscopy

1. INTRODUCTION

Among the portable electronic devices located near or on the body and used to provide intelligent services such as monitoring different signals (heart rate, temperature, etc.), some of them can be integrated to a greater or lesser extent into textile structures in order to develop smart textiles with high added value. One of the main challenge to ensure the development of the smart textile market is to guarantee the power supply of the various electronic components integrated into the textile. Currently, electrical energy is provide by the use of batteries that have a number of disadvantages. One of the alternatives is to develop textile energy harvesting systems. Several effects or phenomena may be involved independently or jointly to ensure energy production. Thus, in recent years the literature mentions the development of textile systems using: i) electromagnetic waves (development of solar cells based on the use of photovoltaic effect [1], development of textile antennas for radiofrequency energy recovery harvesting operating on various bands [2], ii) heat (development of textiles based on the pyroelectric effect [3] or thermoelectric textiles exploiting the Seebeck effect [4], iii) movements (development of triboelectric textiles [5] or piezoelectric textiles [6]).

Polyvinylidene fluoride (PVDF) is commonly used in studies related to the development of piezoelectric energy harvesting textiles. It is a polymorphic polymer with five different crystalline phases, i.e., α , β , γ , γ' , δ and ϵ . Among them, the three main ones are the α - (apolar), β - and γ -phases (polar). Piezoelectricity of PVDF is related to the presence of polar crystalline phases and in particular by the β -phase. In one hand, numerous strategies have been conducted to obtain this latter, i.e., Uni-axial stretching, crystallization under high pressure or high temperature, incorporation of nanofillers, high voltage polarization, etc. In other hand, several methods can be used to evaluate the presence of β -phase into PVDF: differential scanning calorimetry (DSC), dynamic or thermal mechanical analysis (DMA or TMA), X-ray diffraction (XRD) and spectroscopy measurements (FTIR, NMR, Raman). However, these characterizations are performed post-mortem: i.e: after the final stage of the

production process. Among all these tests, Raman spectroscopy is a very interesting analytical tool that provides valuable structural information on various materials, including polymers and that can also be used to made in-situ measurements [7].

In this study, PVDF multifilament yarns dedicated to the development of energy harvesting fabrics are produced by melt spinning. A first trial was performed with five different drawing ratios and the fibers were characterized by post-mortem analyses (DSC, FTIR and Raman spectroscopy measurements). During a second series, on-line measurements were performed by using Raman RXN2 spectrometer from Kaiser Optical Systems. These tests confirm post-mortem measurement but give also complementary informations and in particular on the location of the $\alpha \rightarrow \beta$ transformation during the spinning process.

2. EXPERIMENTAL

2.1 Materials

Polymer - PVDF homopolymer grade, Kynar[®]705 (Arkema, France) in pellet form was used. The following characteristics were given by the supplier: the melt flow index (MFI) is 25 g.10min⁻¹ under a load of 2.16 kg at 220°C, the melting temperature T_m is 173°C and the density is 1.76.

Melt-Spinning of the multifilaments - Two series of PVDF fiber processing were carried out on a Spinboy 1 (Busschaert Engineering, Belgium) spinning pilot to produce multifilament yarns. In the first trial, filaments with different theoretical drawing ratios (DR) from 1.25 to 6 were produced while in the second one dedicated to in situ characterization by Raman spectroscopy, only two drawing ratios were kept, i.e.: 1.25 and 4. PVDF dried pellets were introduced in the feed hopper. The single-screw extruder has the role of melting the polymer and conveying it to the spinnerets (2x40 holes of 1.2 mm diameter) at the temperature of 225°C through a volumetric pump to ensure a defined flow. The resulting multifilament yarn was cooled down by fresh air and coated with spin oil. Then it was drawn between two hot rolls (Alimentation roll - R_1 (110°C) and drawing roll - R_2 (90°C)) by adjusting their rotational speeds to reach the desired drawing ratio. Finally, multifilament yarns were wound on bobbins. The spinning process and the 6 different laser positions (A-F) during on-line Raman measurements are represented on the Figure 1.

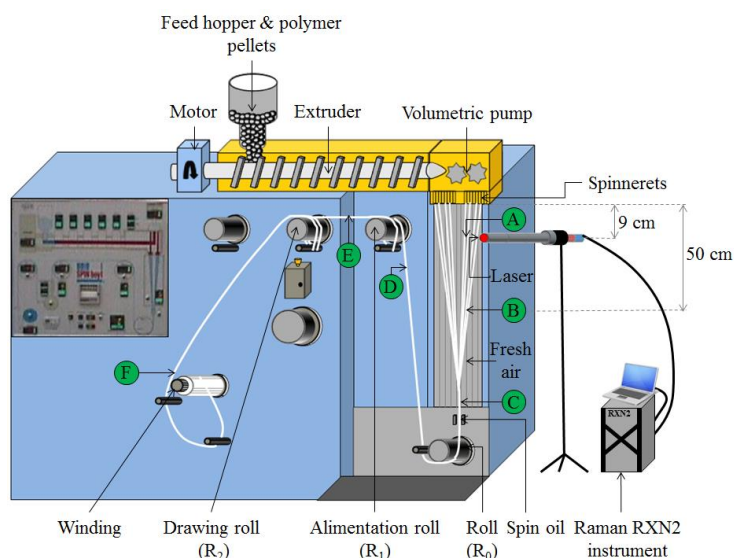


Figure 1. Melt spinning pilot and different positions of the laser (A-F) during Raman in-situ characterization

2.2 Analyses

Post mortem measurements – Thermal characterization was conducted on a Mettler Toledo DSC3+ differential scanning calorimeter in a nitrogen atmosphere (50ml/min) between -60°C and 200°C at a heating rate of 10°C.min⁻¹. Analyses were made on a given amount of knotted fibers (10.0 ± 0.5 mg) sealed into an aluminum pan. Fourier transform infrared spectroscopy was performed using Thermo Nicolet Nexus 470 FTIR system equipped with ATR unit. The fibrous samples were scanned 128 times each between 400 cm⁻¹ and 4000 cm⁻¹ with a resolution of 0.5 cm⁻¹. Post-mortem Raman measurements were carried out by means of a Horiba-LabRam HR Evolution spectrometer with a spectral resolution of 1 cm⁻¹. The 785 nm laser with an intensity of 300 mW was used as the exciting line with a 100x microscope objective and the scattered radiation was detected by a cooled CCD camera. The integration time was 5s and each spectrum was recorded 3 times.

In situ Raman spectroscopy measurements - A Raman RXN2 instrument (Kaiser Optical Systems, USA) was used for in situ monitoring during the second series of PVDF fiber processing on the melt spinning device. The spectrometer was equipped with a laser wavelength of 785 nm and a laser power of 400 mW and offered a spectral resolution of 2 cm⁻¹. Measurements were performed with a non-contact probe provided with a lens of 10 mm focal depth. The integration time for one Raman spectrum was 45s. The Raman laser was moved at 6 different positions. Three of them are located between the extruder and the roller R₀: 9 cm from the spinneret (A), 50 cm from the spinneret (B) and finally before the zone of spin finish application (C). The last three positions are between the roll R₀ and the winding: just before R₁ (D), between R₁ and R₂ (E) and finally before the winding (F).

3. RESULTS AND DISCUSSION

Multifilament yarns produced with 5 different drawing ratios (from DR 1.25 to DR 6) during the first spinning trials were analysed post-mortem. Crystalline phases of PVDF are identified by FTIR and Raman spectroscopy. The form II of PVDF (α) has specific IR absorption bands at 1210, 1149, 975, 795 and 764 cm⁻¹ and Raman vibrational bands at 873 and 795 cm⁻¹. The form I (β) is characterized by a Raman band at 840 cm⁻¹ and IR absorption bands at 1275 cm⁻¹ and a common band at 840 cm⁻¹ with the form III (γ). The IR band at 1234 cm⁻¹ is used to highlight the presence of this latter phase. The figure 2a and 2c show clearly that the characteristic bands of the α -phase decrease as the drawing ratio increase. The disappearance of the low intensity peak at 766 cm⁻¹ and the shoulder at 885 cm⁻¹ in Raman spectra from the DR 4 is an additional sign of the decrease of the α -phase. At the same time, the intensity of the characteristic peaks of the β -phase is greater with the increase in mechanical stresses associated with an increase of the drawing ratios. These results confirm that mechanical stretching is one of the effective methods for assuring $\alpha \rightarrow \beta$ transformation. Shoulders at 1234 and 833 cm⁻¹ for DR 1.25 and DR 2 spectra obtained by IR spectroscopy suggest the presence of γ -phase. The monitoring of crystalline phases by studying endotherms from DSC analyzes is tricky. The melting peaks are dependent on the grade of PVDF used, its mode of transformation, experimental parameters [8] (DSC sample preparation: stripes, knots, bundles of fibers, heating rate, etc.), etc. It is reported that the α - and β -phases present similar melting temperature around 170°C whereas γ -phase have higher melting temperature [9]. Based on the different endotherms recorded during DSC experiments, it can be supposed that all fibers are composed of α - and β -phases. Smaller crystals could be also assigned to the presence of shoulder near the melting peak for the DR 4 and DR 5. The presence of γ -phase does not seem

to be revealed by DSC tests. DSC is therefore mainly used to calculate the crystalline percentage ($\chi_c(\%)$) of the fibers.

$$\chi_c(\%) = \left(\frac{\Delta H}{x_\alpha \Delta H_\alpha + x_\gamma \Delta H_\gamma + x_\beta \Delta H_\beta} \right) \times 100 \quad (1)$$

Where ΔH is the experimental melting enthalpy, ΔH_α , ΔH_γ and ΔH_β are the melting enthalpies of a 100% crystalline sample in the α -, γ -, and β -phases, respectively, x_α , x_γ , x_β and are the amount of the α -, γ -, and β -phases in the sample, respectively, as deduced by FTIR experiments and the method proposed by Cai et al. [10]. A value of 103.4 J.g^{-1} and 93.07 J.g^{-1} are considered for ΔH_β and ΔH_α [11]. The melting enthalpy of γ -phase is assumed identical to that of a 100% α -phase.

The crystallinity, the fraction of electroactive phase ($F_{EA} = \gamma + \beta$ phases), the fraction of the three principal forms of PVDF (F_α , F_β , and F_γ) and the total fraction of β -phase ($F_{\beta\text{total}}$) in the polymer are determined by combining DSC and FTIR analyses and reported in Table 1. Electroactive phase is estimated at 36.6% for the lowest drawing ratio and reaches 75.8% for the highest drawing ratio. Since the complement is totally assigned to the α -phase, the latter strictly follows the opposite trend. For fibers produced with drawing ratios lower or equal to 2, the electroactive phase seems to be mainly composed of γ -phase while for drawing ratio higher than 4 the β -phase is predominant. As illustrated in Figure d, Raman spectra are decomposed in order to separate the contributions of the crystalline phases (α and β) and the amorphous phase. The crystallinity, the ratio between the β and α response, the fraction of β -phase and the total fraction of β -phase in each sample are calculated and summarized in Table 1. This corroborates the previously observed trends and in particular that an $\alpha \rightarrow \beta$ transformation appears as drawing ratio increase.

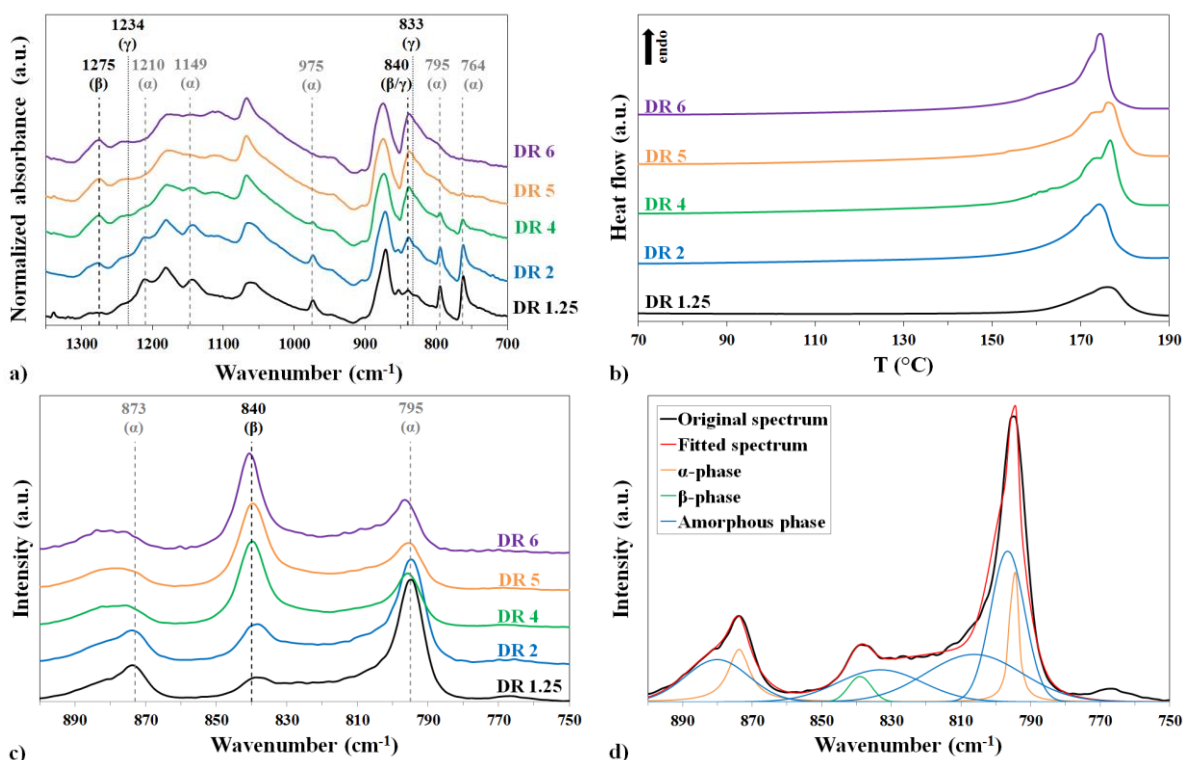
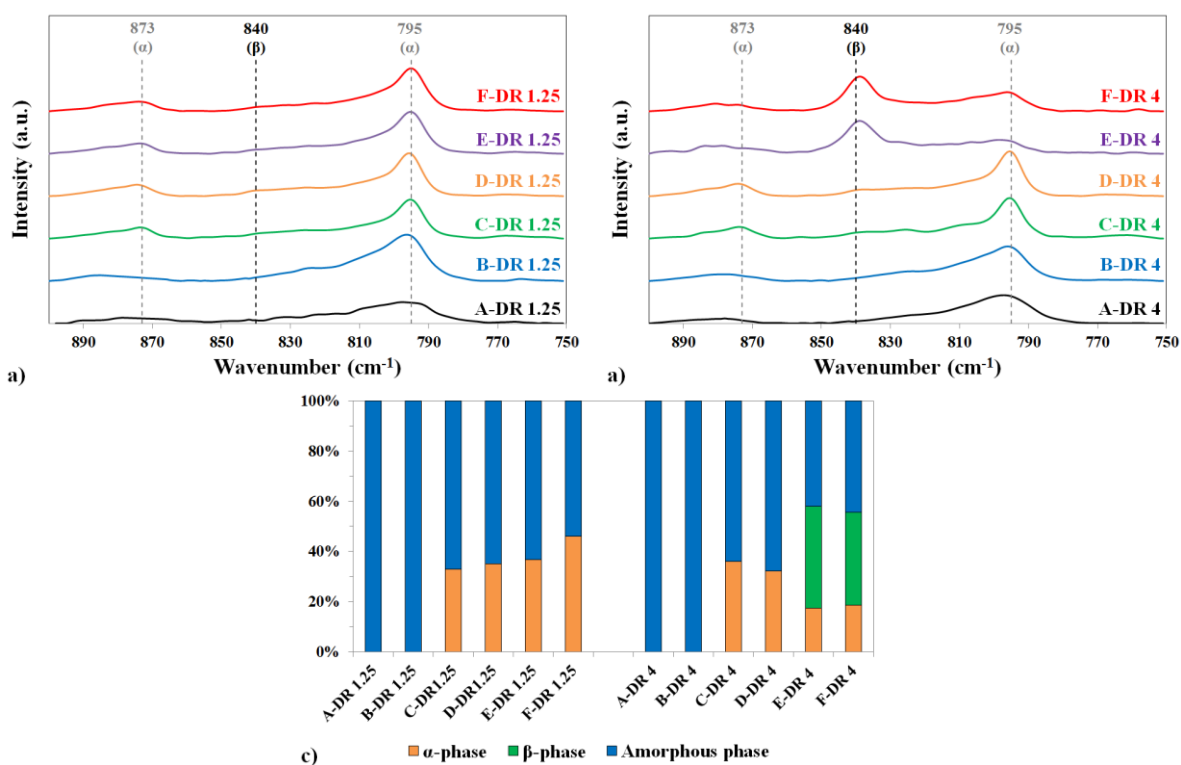


Figure 2. FTIR spectra (a), DSC thermograms (b) and Raman spectra of PVDF fibers with drawing ratios from 1.25 to 6 (c). An example of the Raman spectrum of fiber (DR 1.25) with the deconvolution (d).

Table 1. Data related to the PVDF crystalline phases obtained from DSC, FTIR and Raman experiments

	DSC	FTIR				DSC+FTIR	RAMAN			
	χ_c (%)	F_{EA} (%)	F_α (%)	F_γ (%)	F_β (%)	$F_{\beta total}$ (%)	χ_c (%)	β/α	F_β (%)	$F_{\beta total}$ (%)
DR 1.25	32.2	36.6	63.4	30.7	5.9	1.9	20.8	0.17	14.6	3.0
DR 2	53.0	48.6	51.4	25.4	23.2	12.3	30.8	0.24	19.7	6.1
DR 4	57.4	62.0	38.0	12.5	49.5	28.4	59.0	2.42	70.8	41.8
DR 5	55.4	72.0	28.0	2.8	69.3	38.4	55.7	2.57	72.0	40.1
DR 6	56.7	75.8	24.2	7.3	68.4	38.8	63.3	3.25	76.5	48.4

A new series of tests was conducted focusing on two drawing ratios: a low (DR 1.25) and a higher one (DR 4). The evolution of the crystalline structure was monitored during the process by positioning the laser associated with the Raman spectrometer at 6 different locations on the spinning line. The Raman spectra recorded during the experiments as well as the content of α -, β - and amorphous phases calculated after spectra decomposition are shown in Figure 3. Whatever the drawing ratio considered, no crystalline phase is detectable before the position C. Although both trials (1st: DR 1.25 to DR 6 and 2nd: DR 1.25 and DR 4) were performed with the same parameters, they must be considered independently as variations may occur. For example, sliding on the rolls can cause constraint transfer variations, and theoretical drawing ratios can diverge. Thus, the presence of β -phase in these new filaments produced with a DR 1.25 does not appear. As expected, higher DR causes an increase of the crystallinity and an $\alpha \rightarrow \beta$ transformation that mainly happens at position E between the alimentation roll (R_1) and the drawing roll (R_2).


Figure 3. Raman spectra of PVDF fibers recorded on-line at the 6 different positions for a DR = 1.25 (a) and for a DR = 4 (b). Evolution of amorphous, α - and β -phase at the different positions for the both DR.

4. CONCLUSION

Raman spectroscopy was used to study the crystalline structure of PVDF fibers. This experimental technique allow the identification and quantification of the most relevant phases of PVDF both during post-mortem or for the first time during on-line experiments. This opens new perspectives for fibers optimization by controlling the evolution of the structure when changing process parameters such as the temperatures of the different rollers, etc.

5. ACKNOWLEDGMENTS

Authors are grateful for financial support from BPI France and Arkema to Autonotex Project.

6. REFERENCES

1. A. Bedeloglu, A. Demir, Y. Bozkurt, N. S. Sariciftci, A Photovoltaic Fiber Design for Smart Textiles, *Textile Research Journal*, 2009, Vol. 80, No. 11, 1065–1074.
2. C. Lin, C. Chiu, J. Gong, A Wearable Rectenna to Harvest Low-Power RF Energy for Wireless Healthcare Applications. *11th International Congress on Image and Signal Processing, BioMedical Engineering and Informatics (CISP-BMEI)*, 2018, 1–5.
3. M.-H. You, X.-X. Wang, X. Yan, J. Zhang, W.-Z. Song, M. Yu, Z.-Y. Fan, S. Ramakrishna, Y.-Z. Long, A Self-Powered Flexible Hybrid Piezoelectric–pyroelectric Nanogenerator Based on Non-Woven Nanofiber Membranes, *Journal of Materials Chemistry A*, 2018, Vol. 6, No. 8, 3500–3509.
4. Q. Wu, J. Hu, A Novel Design for a Wearable Thermoelectric Generator Based on 3D Fabric Structure, *Smart Materials and Structures*, 2017, Vol. 26, No. 4, 45037.
5. A. Y. Choi, C. J. Lee, J. Park, D. Kim, Y. T. Kim, Corrugated Textile Based Triboelectric Generator for Wearable Energy Harvesting, *Scientific Reports*, 2017, Vol. 7, 7–12.
6. A. Talbourdet, F. Rault, G. Lemort, C. Cochrane, E. Devaux, C. Campagne, 3D Interlock Design 100% PVDF Piezoelectric to Improve Energy Harvesting, *Smart Materials and Structures*, 2018, Vol. 27, No. 7, 075010.
7. M. T. Riosbaas, K. J. Loh, G. O'Bryan, B. R. Loyola, In Situ Phase Change Characterization of PVDF Thin Films Using Raman Spectroscopy, *Proc. SPIE 9061, Sensors and Smart Structures Technologies for Civil, Mechanical, and Aerospace Systems 2014*, San Diego, USA, 2014, 90610Z.
8. W. Steinmann, S. Walter, M. Beckers, G. Seide, T. Gries, *Applications of Calorimetry in a Wide Context*, Intech, 2013, 277-306.
9. P. Martins, A. C. Lopes, S. Lanceros-Mendez, Electroactive Phases of Poly(vinylidene Fluoride): Determination, Processing and Applications, *Progress in Polymer Science*, 2014, Vol. 39, No. 4, 683–706.
10. X. Cai, T. Lei, D. Sun, L. Lin, A Critical Analysis of the α , β and γ Phases in Poly(vinylidene Fluoride) Using FTIR, *RSC Advances*, 2017, Vol. 7, No. 25, 15382–15389.
11. M. Baqeri, M. M. Abolhasani, M. R. Mozdianfard, Q. Guo, A. Oroumei, M. Naebe, Influence of Processing Conditions on Polymorphic Behavior, Crystallinity, and Morphology of Electrospun poly(Vinylidene Fluoride) Nanofibers, *Journal of Applied Polymer Science*, 2015, Vol. 132, No. 30, 1–11.